



ECG fiducial point extraction using switching Kalman filter

Mahsa Akhbari^{a,b,*}, Nasim Montazeri Ghahjaverestan^a, Mohammad B. Shamsollahi^a, Christian Jutten^b

^a BiSIPL, Department of Electrical Engineering, Sharif university of Technology, Tehran, Iran

^b GIPSA-Lab, Grenoble, and Institut Universitaire de France, France

ARTICLE INFO

Article history:

Received 25 August 2016

Revised 5 January 2018

Accepted 15 January 2018

Keywords:

Electrocardiogram (ECG)

Switching Kalman filter (SKF)

Extended Kalman filter (EKF)

Segmentation

Fiducial point (FP) extraction

ABSTRACT

In this paper, we propose a novel method for extracting fiducial points (FPs) of the beats in electrocardiogram (ECG) signals using switching Kalman filter (SKF). In this method, according to McSharry's model, ECG waveforms (P-wave, QRS complex and T-wave) are modeled with Gaussian functions and ECG baselines are modeled with first order auto regressive models. In the proposed method, a discrete state variable called “switch” is considered that affects only the observation equations. We denote a *mode* as a specific observation equation and *switch* changes between 7 modes and corresponds to different segments of an ECG beat. At each time instant, the probability of each mode is calculated and compared among two consecutive modes and a path is estimated, which shows the relation of each part of the ECG signal to the mode with the maximum probability. ECG FPs are found from the estimated path. For performance evaluation, the Physionet QT database is used and the proposed method is compared with methods based on wavelet transform, partially collapsed Gibbs sampler (PCGS) and extended Kalman filter. For our proposed method, the mean error and the root mean square error across all FPs are 2 ms (i.e. less than one sample) and 14 ms, respectively. These errors are significantly smaller than those obtained using other methods. The proposed method achieves lesser RMSE and smaller variability with respect to others.

© 2018 Elsevier B.V. All rights reserved.

1. Introduction

An electrocardiogram (ECG) describes the electrical activity of the heart. Onset, offset and peak location of ECG waves are known as fiducial points (FPs). Up to now, different methods have been used for detecting the QRS complex. See [1] for a review. These methods are based on mathematical functions, filtering approaches (digital filters [2], adaptive filters [3]), classification methods (neural network approaches [4], support vector machine (SVM) [5], fuzzy C-means algorithm [6]), wavelet transform [7] and empirical mode decomposition (EMD) [8]. Low pass differentiation (LPD) [9], hidden Markov models (HMM) [10–14], partially collapsed Gibbs sampler (PCGS) [15], wavelet transform [16–18], correlation analysis [19,20] and extended Kalman filter (EKF) [21–24] are also used for ECG FP extraction.

FP extraction has been used as a preprocessing step in several applications such as detection of fragmented QRS complex [25],

mobile health care applications [26], “Selvester QRS scoring” system [27], ischemia detection [28], ECG-based subject identification system [29] and biometric recognition based on fusion of ECG and EEG signals [30,31].

Switching state space models are defined as the combination of HMMs and state space models [32]. When the model is linear and additive Gaussian noise exists, the switching state space models are known as “Switching Kalman Filter” (SKF) [33,34]. In the SKF, at each time instance, the states are estimated by several Kalman filters (KFs). Furthermore, a hidden discrete state variable called *switch* is considered whose status changes over the time according to a Markov model. The switch indicates the KF which estimates the states better than others.

SKF is used for several applications such as figure tracking [35], acoustic segmentation [36], contour tracking in clutter [37], modeling and detecting motor cortical activity [38], prediction and tracking an adaptive meteorological sensing network [39], tracking and event detection at traffic intersections [40], ECG ventricular beat classification [41] and finally for apnea bradycardia detection from ECG signals [42].

Although the methods based on dynamic models (EKF) [24] and sequential methods (HMM) [14] have been used for ECG FP extrac-

* Corresponding author at: BiSIPL, Department of Electrical Engineering, Sharif university of Technology, Tehran, Iran.

E-mail addresses: akhbari.mahsa@gmail.com, mahsa_akhbari@ee.sharif.edu (M. Akhbari), montazeri.nasim@gmail.com (N.M. Ghahjaverestan), mbshams@sharif.edu (M.B. Shamsollahi), christian.jutten@gipsa-lab.grenoble-inp.fr (C. Jutten).

tion, the methods based on SKF (which is combination of KF and HMM methods) have not been used for this application yet. The goal of this paper is showing the ability of SKF-based methods for ECG FP extraction.

In [21–24], methods based on EKF have been proposed. The main limitation of such methods is their sensitivity to the initial location of the Gaussian functions as well as initial parameters of EKF, that must be defined by the user. Conversely, one of the advantages of the proposed SKF model is that it is not sensitive to the initial location of Gaussian functions and initial parameters of SKF.

According to McSharry's model [43], ECG waves (P-wave, QRS complex and T-wave) are modeled with Gaussian functions. Baselines and segments between ECG waves are modeled with first order autoregressive (AR) models. In this SKF approach, a discrete switch affects only the observation equations and switches between 7 different values related to the 3 waves and the 4 baseline segments.

The performance of the proposed method is compared with previously published methods, including Wavelet [17], PCGS [15] and EKF-based method (EKF17) [22]. We also have a comparison with our previously proposed methods (linear and nonlinear EKF25 [23,24]). Validation and comparison are done over Physionet QT database [44,45].

The paper is organized as follows: ECG dynamical model and details of SKF approach for ECG FP extraction are described in Section 2. Section 3 presents the experimental results, and finally Section 4 concludes the paper.

2. Methods

In this section, we first present the ECG model we used and then we fully describe the proposed SKF method.

2.1. ECG Kalman filtering framework

McSharry et al. [43] have proposed a synthetic ECG generator which is based on a nonlinear dynamic model. Sameni et al. [46] transformed it into polar coordinates from Cartesian coordinates and proposed an EKF-based framework which has two state variables and two corresponding observations. The discrete state-equations of this model are as follows:

$$\begin{cases} \varphi_{k+1} = (\varphi_k + \omega_k \delta) \bmod(2\pi) \\ z_{k+1} = -\sum_i \delta \frac{\alpha_{ik} \omega_k}{b_{ik}^2} \Delta \theta_{ik} \exp\left(-\frac{\Delta \theta_{ik}^2}{2b_{ik}^2}\right) + z_k + \eta_k \end{cases} \quad (1)$$

where k denotes the discrete time, φ_k is the phase of ECG and ω_k is the beat-to-beat angular frequency of the RR interval. In this model, z_k is a state variable which is the sum of 5 Gaussian functions ($i \in \{P, Q, R, S, T\}$) and represents estimated amplitude of ECG. Each Gaussian function is defined with three parameters: α_{ik} , b_{ik} and θ_{ik} , which correspond to the amplitude, width and location of the Gaussian functions and $\Delta \theta_{ik} = (\varphi_k - \theta_{ik}) \bmod(2\pi)$; δ is the sampling period and η_k models the inaccuracies of the dynamic model.

2.2. Proposed dynamic model

For an ECG beat, we can define seven segments: B_1 , P, PQ (B_2), QRS, ST (B_3), T and B_4 which are shown in Fig. 1. In the proposed model, we consider separate states for P-wave, QRS complex and T-wave which are modeled with Gaussian functions. We also assign a state defined with a first order AR model to each baseline (B_1 , B_2 , B_3 and B_4). Similar to previous EKF-based models, we also consider the phase of ECG as a state. Hence, a model with 8 states

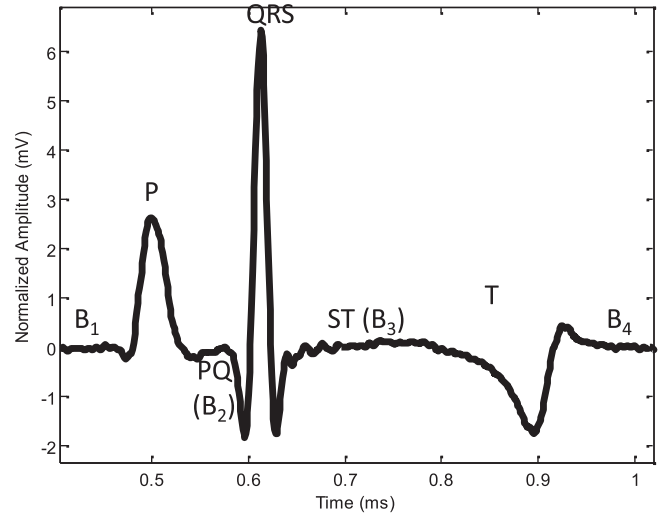


Fig. 1. Segments of a single ECG beat.

is generated. In fact, although segments B_1 and B_4 are almost similar, since we find the fiducial points for each beat separately, we consider two separate segments B_1 and B_4 . Discrete state and observation equations of this model are defined in (2) and (3), respectively. We use “C” to denote the QRS complex. In (2), for simplicity we consider that the coefficients of AR models are equal to one ($a_{B_1} = a_{B_2} = a_{B_3} = a_{B_4} = 1$) but in general, other values smaller and very close to 1 can be examined.

$$\begin{cases} \varphi_{k+1} = (\varphi_k + \omega_k \delta) \bmod(2\pi) \\ B_{1,k+1} = a_{B_1} B_{1,k} + \eta_{B_{1,k}} \\ P_{k+1} = -\frac{\delta \alpha_{P,k} \omega_k}{b_{P,k}^2} \Delta \theta_{P,k} \exp\left(-\frac{\Delta \theta_{P,k}^2}{2b_{P,k}^2}\right) + P_k + \eta_{P_k} \\ B_{2,k+1} = a_{B_2} B_{2,k} + \eta_{B_{2,k}} \\ C_{k+1} = -\sum_{i \in \{Q,R,S\}} \delta \frac{\alpha_{ik} \omega_k}{b_{ik}^2} \Delta \theta_{ik} \exp\left(-\frac{\Delta \theta_{ik}^2}{2b_{ik}^2}\right) + C_k + \eta_{C_k} \\ B_{3,k+1} = a_{B_3} B_{3,k} + \eta_{B_{3,k}} \\ T_{k+1} = -\frac{\delta \alpha_{T,k} \omega_k}{b_{T,k}^2} \Delta \theta_{T,k} \exp\left(-\frac{\Delta \theta_{T,k}^2}{2b_{T,k}^2}\right) + T_k + \eta_{T_k} \\ B_{4,k+1} = a_{B_4} B_{4,k} + \eta_{B_{4,k}} \end{cases} \quad (2)$$

$$\begin{cases} \Phi_k = \varphi_k + \nu_{1k} \\ z_k = B_{1,k} + P_k + B_{2,k} + C_k + B_{3,k} + T_k + B_{4,k} + \nu_{2k} \end{cases} \quad (3)$$

In (2), the first state is the phase of the ECG. States 3, 5 and 7 are distinct ECG waveforms. The ECG baselines are considered as the 2nd, 4th, 6th and 8th state variables. The system state and process noise vectors are defined as:

$$\begin{aligned} \underline{x}_k &= [\varphi_k, B_{1,k}, P_k, B_{2,k}, C_k, B_{3,k}, T_k, B_{4,k}]^T \\ \underline{w}_k &= [\alpha_{ik}, b_{ik}, \theta_{ik}, \omega_k, \eta_{jk}]^T \\ i &\in \{P, Q, R, S, T\}, \quad j \in \{B_1, P, B_2, C, B_3, T, B_4\}. \end{aligned} \quad (4)$$

In (3), the first observation is a linearly approximated phase of ECG beat, and z_k is the recorded ECG which can be considered as the sum of $B_{1,k}$, P_k , $B_{2,k}$, C_k , $B_{3,k}$, T_k and $B_{4,k}$ states in the model. Observation and measurement noise vectors are defined, respectively, as: $\underline{y}_k = [\Phi_k, z_k]^T$ and $\underline{v}_k = [\nu_{1k}, \nu_{2k}]^T$.

2.3. SKF-based ECG model

In our proposed SKF, we assume that the switch only affects the observation equation. We then denote a *mode* as a specific observation equation and the switch s is a discrete state which changes between 7 modes, $j = 1, 2, \dots, 7$. We assume to have a first order Markov chain whose matrix transition denotes as Z where $z_{ij} = P(s_k = j | s_{k-1} = i)$. The Markov chain has left-to-right structure i.e. $z_{ij} \neq 0$ if and only if $j = i$ or $j = i + 1$ or ($j = 7$ and $i = 1$). Since the model which is defined in (2) is nonlinear, in order to use a Kalman filter for this system, it is necessary to derive a linear approximation of it near desired reference points (\hat{x}_k, \bar{w}_k) and (\hat{x}_k^-, \bar{v}_k) . This approximation will lead to the following linear estimate:

$$\begin{cases} \underline{x}_{k+1} = f(\underline{x}_k, \underline{w}_k, k) \approx f(\hat{x}_k, \bar{w}_k, k) + A_k(\underline{x}_k - \hat{x}_k) + D_k(\underline{w}_k - \bar{w}_k) \\ \underline{y}_k = g(\underline{x}_k, \underline{v}_k, k) \approx g(\hat{x}_k^-, \bar{v}_k, k) + H_k(\underline{x}_k - \hat{x}_k^-) + G_k(\underline{v}_k - \bar{v}_k) \end{cases} \quad (5)$$

where

$$\begin{aligned} A_k &= \frac{\partial f(\underline{x}_k, \underline{w}_k, k)}{\partial \underline{x}_k} \Big|_{\underline{x}_k = \hat{x}_k, \underline{w}_k = \bar{w}_k}, & D_k &= \frac{\partial f(\underline{x}_k, \underline{w}_k, k)}{\partial \underline{w}_k} \Big|_{\underline{x}_k = \hat{x}_k, \underline{w}_k = \bar{w}_k} \\ H_k &= \frac{\partial g(\underline{x}_k, \underline{v}_k, k)}{\partial \underline{x}_k} \Big|_{\underline{x}_k = \hat{x}_k^-, \underline{v}_k = \bar{v}_k}, & G_k &= \frac{\partial g(\underline{x}_k, \underline{v}_k, k)}{\partial \underline{v}_k} \Big|_{\underline{x}_k = \hat{x}_k^-, \underline{v}_k = \bar{v}_k} \end{aligned} \quad (6)$$

The state and observation equations of the proposed SKF can be written as:

$$\begin{aligned} \underline{x}_{k+1} &= A_k \underline{x}_k + D_k \underline{w}_k \\ \underline{y}_k &= H_k^{(j)} \underline{x}_k + G_k \underline{v}_k^{(j)} \end{aligned} \quad (7)$$

where $H_k^{(j)}$ and $\underline{v}_k^{(j)}$ are the observation matrix and observation noise of the j th mode, respectively. Elements of A_k and D_k matrices are defined in (A.1) and (A.2), respectively, in Appendix A. Here, the matrices A_k , D_k and $Q_k = Cov(\underline{w}_k)$ are not changed for different modes. The dimension of $H_k^{(j)}$ is 2×8 and its nonzero elements are defined in (8):

$$\begin{cases} H_k^{(j)}(1, 1) = 1, & j = 1, 2, \dots, 7 \\ H_k^{(j)}(2, j + 1) = 1, & j = 1, 2, \dots, 7 \end{cases} \quad (8)$$

This means that the observation equation has linear dynamics at each time instant but it is time variant and switches among several linear equations over the time. $\underline{v}_k^{(j)} = [v_{1k}, v_{2k}]^T$ is the observation noise vector. The noise covariance matrix $R_k^{(j)} = Cov(\underline{v}_k^{(j)})$ is defined from the observations of the j th mode. Matrix G_k is constant for the different values of the switch: $G_k = I_2$ (identity matrix of size 2), $G_k \underline{v}_k^{(j)} = \underline{v}_k^{(j)}$ and $G_k R_k^{(j)} G_k^T = R_k^{(j)}$.

2.4. Procedure of SKF-based FP extraction

At each time instant k , the probability of each mode is calculated as: $K_k^j = P(s_k = j | \underline{y}_{1:k})$, $j \in \{1, 2, \dots, 7\}$. If K_k^j has the maximum value at time k , the observation at time k is likely generated by j th mode. Monitoring the value of the parameter K_k^j , $j \in \{1, 2, \dots, 7\}$ for each mode allows us to choose the optimal mode. Therefore in this work, we perform SKF and monitor K_k^j .

We use 2-fold cross validation [47] for each record (the records which are used in this paper will be explained in Section 2.5). Initial values for \underline{x}_0^i , P_0^i , Q_0 , $H_0^{(j)}$, $R_0^{(j)}$, K_0^i and Z_0 ($i, j = 1, 2, \dots, 7$) are found from train data in the Initialization step. \underline{x}_0^i is the initial estimation of state and P_0^i is its covariance matrix. Q_0 , $H_0^{(j)}$, $R_0^{(j)}$ and K_0^i are initial values for Q_k , $H_k^{(j)}$, $R_k^{(j)}$ and K_k^i , respectively. Finally,

Z_0 is the initial value of matrix Z where $z_{ij} = P(s_k = j | s_{k-1} = i)$. In [41,48], the estimation of the covariance matrix is done by performing a random search on the training data in order to optimize the covariance matrix parameters. In this work, for defining the initial location of the Gaussians, we follow the same procedure of Sameni et al. [46]. we choose manually the initial location of the Gaussians and then doing a curve fitting. For estimation of the covariance matrices, we follow the same procedure as [46].

Here, since the matrices A_k , D_k and Q_k are not changed for different modes, the training step includes only the initialization step and no parameter is trained in this step. After that we perform inference procedure (in one iteration) as shown in Algorithm 1, below. Functions *filter*, *StatesProbability* and *Collapse* and their parameters are defined in Appendix B.

Algorithm 1 SKF: Inference

Inputs: \underline{x}_0^i , P_0^i , Q_0 , $H_0^{(j)}$, $R_0^{(j)}$, K_0^i and Z_0 , $i, j = 1, 2, \dots, 7$.

Outputs: K_k^j

- 1: **for** $k = 1, 2, \dots, T$ **do**
 - 2: Compute A_k and D_k from (A.1) and (A.2) in Appendix A.
 - 3: **for** $i, j = 1, 2, \dots, 7$ **do**
 - 4: $[\underline{x}_k^{ij}, P_k^{ij}, L_k^{ij}] = filter(\underline{x}_{k-1}^i, P_{k-1}^i, A_k, D_k, Q_k, H_k^{(j)}, R_k^{(j)})$
 - 5: $[K_k^{ij}, K_k^j, g_k^{ij}] = StatesProbability(L_k^{ij}, z_{ij}, K_{k-1}^i)$
 - 6: $[\underline{x}_k^j, P_k^j] = Collapse(\underline{x}_k^{ij}, P_k^{ij}, K_k^j, g_k^{ij})$
 - 7: **end for**
 - 8: **end for**
 - 9: Applying a threshold on K_k^j
-

In the function *filter*, $\underline{x}_k^{-ij} = E\{\underline{x}_k | \underline{y}_{1:k-1}, s_k = j, s_{k-1} = i\}$ is the prior estimate of the state vector, in the k th stage, using the past observations \underline{y}_0 to \underline{y}_{k-1} and $\underline{x}_k^{ij} = E\{\underline{x}_k | \underline{y}_{1:k}, s_k = j, s_{k-1} = i\}$ is the posterior estimate of this state vector after adding the k th observations \underline{y}_k . P_k^{-ij} and P_k^{ij} are defined in the same manner to be the prior and posterior estimates of the covariance matrices, in the k th stage, before and after using the k th observation, respectively. $L_k^{ij} = P(\underline{y}_k | \underline{y}_{1:k-1}, s_k = j, s_{k-1} = i)$ is the likelihood of observing the k th observation \underline{y}_k .

The function *StatesProbability*, computes the probabilistic parameters $K_k^j = P(s_k = j | \underline{y}_{1:k})$, $g_k^{ij} = P(s_{k-1} = i | \underline{y}_{1:k}, s_k = j)$ and $K_{k-1}^i = P(s_{k-1} = i, s_k = j | \underline{y}_{1:k}) = K_k^j g_k^{ij}$.

Finally, the function *Collapse* approximates mixture of Gaussians as a unique Gaussian by moment matching. The mean vector and covariance matrix of the unique Gaussian are the same as that of the mixture and are computed as: $\underline{x}_k^j = E\{\underline{x}_k | \underline{y}_{1:k}, s_k = j\}$ and $P_k^j = Cov\{\underline{x}_k | \underline{y}_{1:k}, s_k = j\}$ from mixture model using an approximation of $p(\underline{x}_k | \underline{y}_{1:k}, s_k = j) = \mathcal{N}(\underline{x}_k^j, P_k^j)$. More information about SKF functions can be found in [38,42].

The procedure of finding K_k^j is done for each ECG beat, separately. Since each ECG beat starts with B_1 segment, we assume that $K_0^1 = 1$ and $K_0^i = 0$, $i = 2, \dots, 7$.

For each time instant k , K_k^j has seven values according to the values which the switch can obtain. Since switch s has a left-to-right HMM model, we find the optimum mode between two consecutive modes by:

$$mode_{opt} = \underset{j}{\operatorname{argmax}} K_k^j, \quad j = \{kk, kk + 1\}, \quad kk \in \{1, 2, \dots, 6\} \quad (9)$$

Where kk is the current state. After finding the “ $mode_{opt}$ ” values, a path is estimated from these values. The estimated path has seven levels, each one associated to one segment. Levels 1–7 represent the B_1 , P, B_2 , QRS, B_3 , T and B_4 segments, respectively, (like Fig. 3).

The proposal to find the onset and offset of waves from the estimated path is as follows:

- P_{on} : the point in which the path transits from levels 1 to 2
- P_{off} : the point in which the path transits from levels 2 to 3
- QRS_{on} : the point in which the path transits from levels 3 to 4
- QRS_{off} : the point in which the path transits from levels 4 to 5
- T_{on} : the point in which the path transits from levels 5 to 6
- T_{off} : the point in which the path transits from levels 6 to 7

Since the peaks can be positive or negative, peak position of waves (P_{peak} , R_{peak} , T_{peak}) are defined as the maximum of absolute value of signal between onset and offset.

2.5. Data and evaluation metrics

To evaluate the performance of the proposed method in extracting ECG fiducial points, we need ECG recordings annotated by physicians. Thus, we use records of Arrhythmia, Normal Sinus Rhythm, ST Change and Supraventricular databases which are annotated in the Physionet QT database (32 records) [44,45]. The records are sampled at 250 Hz (4 ms between 2 successive samples) and each of them has 30–50 annotated beats. Totally we use 975 annotated beats for evaluation of the performance of the methods.

We use 2-fold cross validation for each record and the initial parameters of SKF model are found from train data.

For quantitative evaluation of a FP extraction method, we calculate the estimation error defined as time differences between estimated points by proposed method and cardiologist annotations (considered as ground truth). Quantitative results are reported using common metrics: mean (m), standard deviation (sd) and root mean square error (RMSE), defined as follows:

$$RMSE = \sqrt{MSE} = \sqrt{\frac{1}{N} \sum_{i=1}^N (e_i)^2} = \sqrt{(m^2 + sd^2)} \quad (10)$$

where $e_i = \hat{y}_i - y_i$ is denoted as the i th element of the estimation error vector and N is the length of error vector. y_i and \hat{y}_i are the i th cardiologist annotation and estimated point, respectively. m , sd and $RMSE$ are given in ms. Since $RMSE$ considers mean and standard deviation of error, it is a more relevant parameter for comparing methods.

3. Results

Fig. 2 shows how the estimated path is obtained from comparing the values of K_k^j parameter. In this figure, the upper subfigure shows the calculated K_k^j , $j = 1, \dots, 7$ probabilities for one beat. We can see that for example K_k^1 has high value on the segment which is related to B_1 segment and has low (almost zero) value in other segments and so on. By comparing the two consecutive K_k^j values by (9), we can obtain the $mode_{opt}$ and the estimated path which is plotted in lower subfigure in Fig. 2.

Fig. 3 shows the estimated path by the SKF for a small segment of the record 231 of the QT database. The colorful vertical lines show the original location of FPs which are annotated by a physician and the multilevel path is estimated by the proposed SKF. This figure is an illustrative example of what the estimated path looks like and clarify how the onset and offset of waves can be found from the transition of one level to upper level in a multi-level estimated path.

Here, we first present the quantitative results of proposed SKF for some records with different morphologies. After that, we compare the estimation error of SKF and other methods.

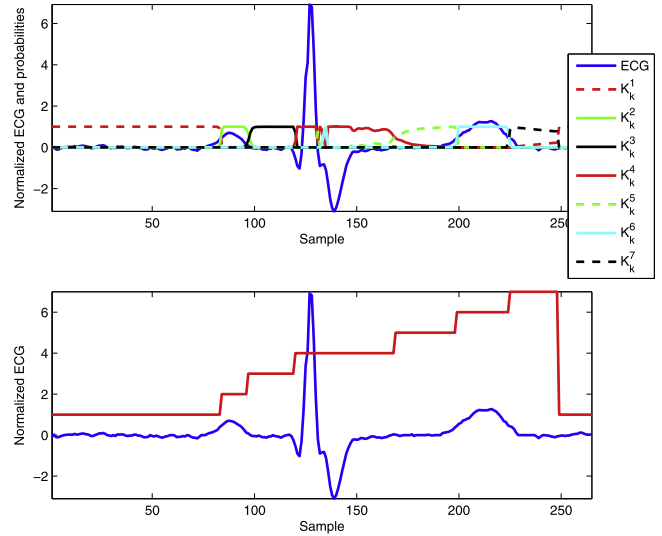


Fig. 2. The K_k^j values and estimated path by SKF for record Sel231.

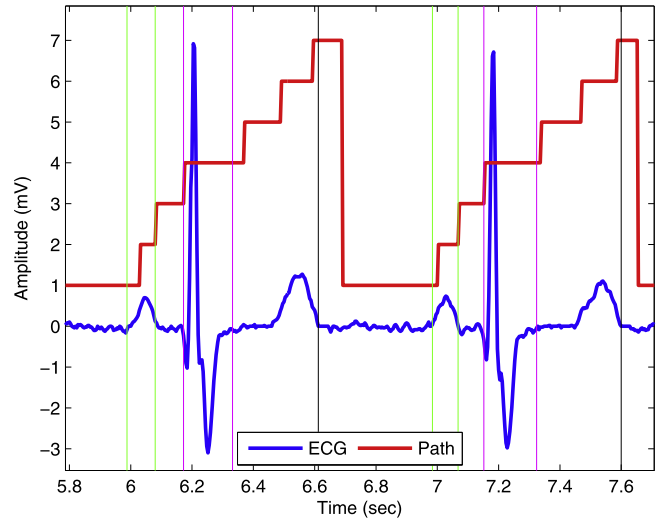


Fig. 3. Original labels and estimated path by SKF for record Sel231.

Fig. 4 shows the original and estimated FPs for sel41 of the QT database. In this figure, the estimated onset, peak and offset of P- and T-waves are denoted by stars and original labels of physician are denoted by vertical lines. This record is a sudden death record and has negative R-peak and broad P- and T-waves. And also the P-wave of one beat starts suddenly after ending the T-wave of previous beat. We can see that for this record, the proposed SKF can estimate the fiducial points accurately.

Fig. 5 shows the original and estimated FPs for sel808 of the QT database. This record is a supra-ventricular record and has normal P-wave and inverted T-wave. We can see that SKF has good performance for this record.

Fig. 6 shows the original and estimated FPs for Sel301 of the QT database. This record is a ST-change record and has bi-phasic T-wave with negative and positive peaks. The physician considers the positive peak as the annotated peak. We can see that SKF estimates the peak and offset of T-waves accurately.

Finally, Fig. 7 shows the original and estimated FPs for Sel233 of the QT database. This record is an arrhythmia record and has neg-

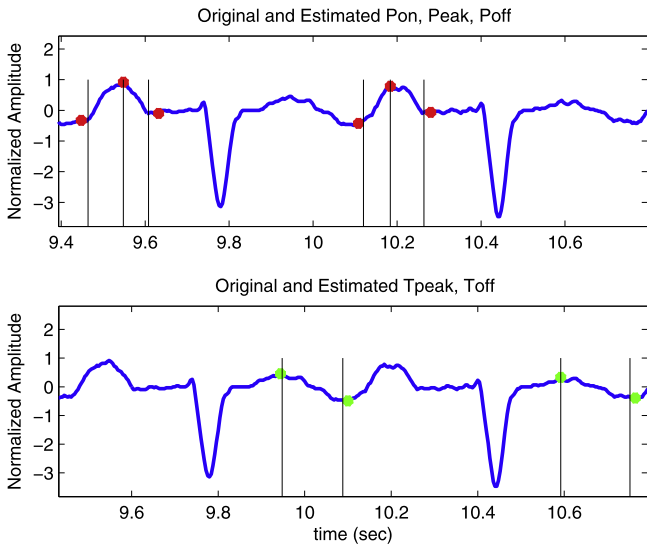


Fig. 4. Original and estimated onset, peak and offset of P- and T-waves by SKF for record Sel41.

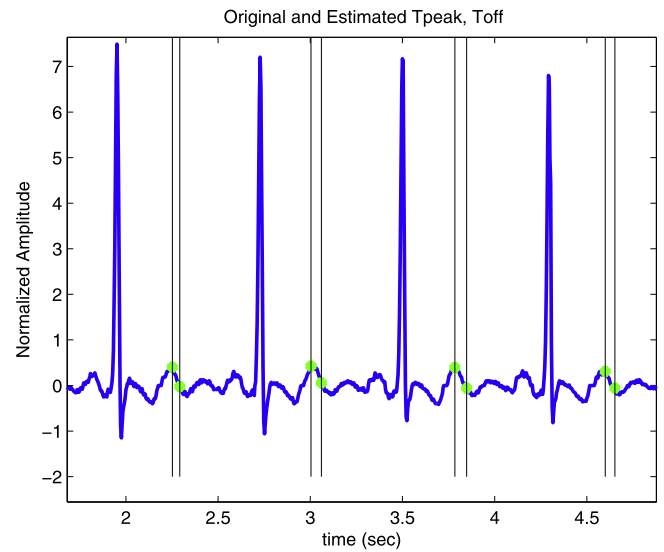


Fig. 6. Original and estimated peak and offset of T-waves by SKF for record Sel301.

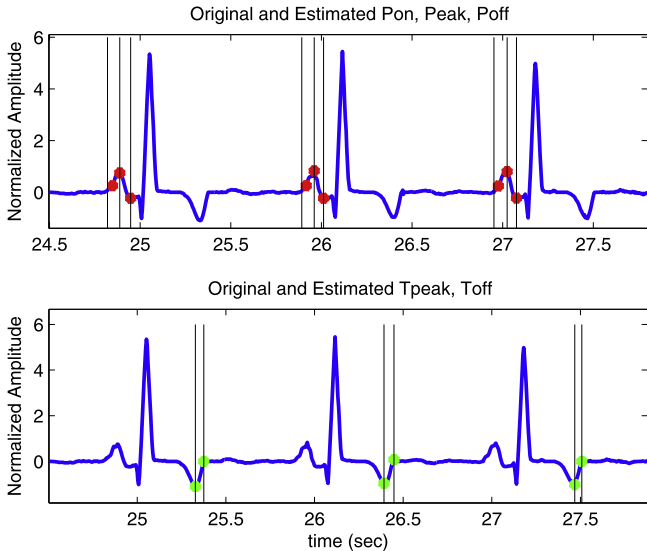


Fig. 5. Original and estimated onset, peak and offset of P- and T-waves by SKF for record Sel808.

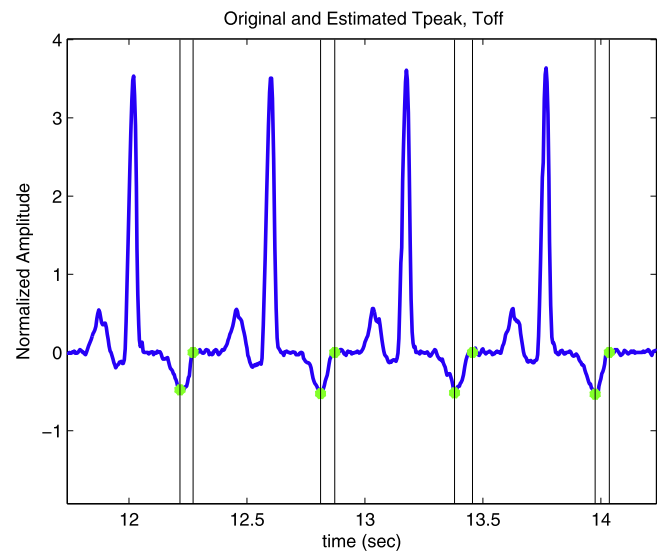


Fig. 7. Original and estimated peak and offset of T-waves by SKF for record Sel233.

ative T-wave. We can see that the proposed SKF has good results for the peak and offset of T-waves.

The quantitative results of different methods for ECG FP extraction for 32 records of QT database are compared in Tables 1 and 2. In Table 1, we compare the proposed SKF method with other methods of the literature: Wavelet [17], PCGS [15] and EKF-based method (EKF17) [22]. In Table 2, we compare SKF with our previously proposed methods based on EKF: linear and nonlinear EKF25 methods proposed in [23] and [24]. Most of the records of QT database do not have reference label for T_{on} . Our proposed method can estimate the location of T_{on} but we cannot report the results of estimation error for T_{on} due to lack of reference labels.

According to the results of Table 1, the mean errors of the SKF method for all FPs except P_{on} are smaller than or around two samples (8 ms). The standard deviations are around four to five samples for the onset and offset of waves and around one sample for the peak of waves.

In Table 1, the best results of RMSE values among four rows are highlighted as bold. We observe that the RMSE values of the SKF method for all FPs except P_{off} are less than other methods, especially for T_{off} . And also the estimation error by SKF for P_{off} is less than estimation error achieved by PCGS and EKF17.

The mean and standard deviation of estimation error across all FPs are estimated for SKF, Wavelet, PCGS and EKF17 methods as 2.2 ± 13.7 , 1.9 ± 26.2 , 5.5 ± 38 and 6 ± 36.2 ms, respectively. RMSE values across all FPs are estimated for above-mentioned methods as 14, 23, 35 and 37 ms, respectively. We observe that the standard deviation and RMSE values for the SKF are smaller than the other methods: it means that the method presented in this paper can find FPs more accurately than other existing methods.

We also compared the proposed SKF method with our previously proposed methods (linear and nonlinear EKF25 methods) in Table 2. The results show that for all FPs except P_{on} , P_{off} and QRS_{off} , SKF has better results than EKF25 methods.

Table 1

Mean \pm standard deviation (first line) and RMSE (second line) of error in ms between estimated FPs and manual annotations for signals of the QT database ($f_s=250$ Hz), (N.A.: not available).

Method	P_{on}	P_{peak}	P_{off}	QRS_{on}	R_{peak}	QRS_{off}	T_{peak}	T_{off}
SKF	23.4 \pm 15.2 27.8	-0.1 \pm 1.5 1.5	-6.4 \pm 20 21	6.6 \pm 10.2 12	0.01 \pm 0.1 0.1	-5.7 \pm 8.5 10.3	-0.01 \pm 0.4 0.4	0.6 \pm 10.8 10.8
Wavelet [17]	-2.3 \pm 31.6 31.7	0.7 \pm 25 25	2.6 \pm 15.2 15.4	12.4 \pm 13.6 18.4	1.4 \pm 3.6 3.8	1.9 \pm 13.8 13.9	7.5 \pm 27.5 28.5	7.3 \pm 32.2 33
PCGS [15]	-30 \pm 29.4 42	5.2 \pm 8.3 9.8	21.1 \pm 15.5 26.2	N.A. N.A.	N.A. N.A.	N.A. N.A.	2.6 \pm 29.7 29.8	27.5 \pm 44 51.8
EKF17 [22]	-11 \pm 28.7 30.7	9 \pm 19.2 21.2	27.4 \pm 23.5 36.1	-24.5 \pm 39.2 46.2	4.5 \pm 6.4 7.8	22.2 \pm 40.6 46.2	-4.6 \pm 34 34.3	24.8 \pm 44.5 51

Table 2

Mean \pm standard deviation (first line) and RMSE (second line) of error in ms between estimated FPs and manual annotations for signals of the QT database ($f_s=250$ Hz), Methods: SKF, Linear EKF25 (L. EKF25) and Nonlinear EKF25 (N. EKF25).

Method	P_{on}	P_{peak}	P_{off}	QRS_{on}	R_{peak}	QRS_{off}	T_{peak}	T_{off}
SKF	23.4 \pm 15.2 27.8	-0.1 \pm 1.5 1.5	-6.4 \pm 20 21	6.6 \pm 10.2 12	0.01 \pm 0.1 0.1	-5.7 \pm 8.5 10.3	-0.01 \pm 0.4 0.4	0.6 \pm 10.8 10.8
L. EKF25 [23]	0.9 \pm 14.7 14.8	4 \pm 10.9 11.6	-0.1 \pm 11.7 11.7	0.55 \pm 12.3 12.3	1.5 \pm 2.7 3.1	-2.5 \pm 7 7.3	-0.6 \pm 9.7 9.7	0.3 \pm 14.7 14.7
N. EKF25 [24]	-1.9 \pm 26.7 26.8	3.4 \pm 15 15.4	-1.6 \pm 13.4 13.5	1 \pm 12.7 12.7	1.2 \pm 5.3 5.5	-1.7 \pm 7 7.2	-1 \pm 8.8 8.8	-0.4 \pm 11.5 11.5

The simulations were done using a system with Core i3, 2.53 GHz CPU. The run-time of the SKF method for one second record takes about 3 s.

4. Discussion and conclusions

In this paper, a novel method based on SKF for ECG fiducial point extraction is proposed. Experiments carried out on ECG signals from the QT database show that the SKF performance is similar or better than the state of the art ECG delineators such as EKF17, PCGS and Wavelet. For most of FPs, SKF outperforms linear and nonlinear EKF25 methods.

The main contribution of this paper is proposing a SKF model for ECG FP extraction, which for each ECG wave or segment, a separate state is considered. ECG waves are modeled as a sum of 5 Gaussian functions and ECG baselines are modeled with a first order AR model. The switch only affects the observations. We used 2-fold cross validation and the initial parameters are found from train data. In the test step, the probability of $K_k^j = P(s_k = j | y_{1:k})$ is compared among all modes and a path is estimated, which shows the relation of each part of the ECG signal to the mode with the maximum probability. FPs are directly found from the obtained path.

EKF-based approaches have been previously used for ECG FP extraction [21–24]. The main limitation of such methods is their sensitivity to the initial location of the Gaussian functions as well as initial parameters of EKF, that must be defined by the user. HMM-based approaches have also been previously proposed for ECG FP extraction [10–13]. In these methods, defining a suitable HMM structure, training step and finding the HMM parameters are very critical and methods are sensitive to these points.

The advantages of the proposed SKF model are: (i) it is sensitive neither to the initial location of the Gaussian functions nor to the initial parameters of SKF, (ii) it does not require severe training step.

The main goal of this paper, is to show the ability of SKF-based methods for ECG FP extraction. The complexity analysis and adapting the algorithm for real-time application are not in the scope of the paper and can be considered as future works.

Acknowledgment

This work has been partly supported by the Ph.D. scholarship of the French Embassy.

Appendix A. EKF matrices derivations

In order to set up an EKF model based on the nonlinear synthetic model of (2), it is necessary to have a linearized version of the model. Consequently, the state-equation of (2) requires linearization using (5) and (6). The following equations represent the linearized model with respect to the state variables (non-zero elements of matrix A_k):

$$\begin{aligned}
 A_k(1, 1) &= A_k(2, 2) = A_k(3, 3) = A_k(4, 4) = A_k(5, 5) = A_k(6, 6) \\
 &= A_k(7, 7) = 1 \\
 A_k(3, 1) &= -\delta \frac{\alpha_{P,k} \omega_k}{b_{P,k}^2} \left[1 - \frac{\Delta \theta_{P,k}^2}{b_{P,k}^2} \right] \exp \left(-\frac{\Delta \theta_{P,k}^2}{2b_{P,k}^2} \right) \\
 A_k(5, 1) &= -\sum_{i \in \{Q,R,S\}} \delta \frac{\alpha_{ik} \omega_k}{b_{ik}^2} \left[1 - \frac{\Delta \theta_{ik}^2}{b_{ik}^2} \right] \exp \left(-\frac{\Delta \theta_{ik}^2}{2b_{ik}^2} \right) \\
 A_k(7, 1) &= -\delta \frac{\alpha_{T,k} \omega_k}{b_{T,k}^2} \left[1 - \frac{\Delta \theta_{T,k}^2}{b_{T,k}^2} \right] \exp \left(-\frac{\Delta \theta_{T,k}^2}{2b_{T,k}^2} \right)
 \end{aligned} \tag{A.1}$$

Similarly, the linearization of (2) with respect to the process noise components yields (the non-zero elements of matrix D_k):

$$\begin{aligned}
 D_k(1, 16) &= \delta, D_k(2, 17) = D_k(4, 19) = D_k(6, 21) = D_k(8, 23) = 1 \\
 D_k(3, 18) &= D_k(5, 20) = D_k(7, 22) = 1 \\
 D_k(3, 1) &= -\delta \frac{\omega_k \Delta \theta_{P,k}}{b_{P,k}^2} \exp\left(\frac{-\Delta \theta_{P,k}^2}{2b_{P,k}^2}\right) \\
 D_k(3, 6) &= 2\delta \frac{\alpha_{P,k} \omega_k \Delta \theta_{P,k}}{b_{P,k}^3} \left(1 - \frac{\Delta \theta_{P,k}^2}{2b_{P,k}^2}\right) \exp\left(\frac{-\Delta \theta_{P,k}^2}{2b_{P,k}^2}\right) \\
 D_k(3, 11) &= \delta \frac{\alpha_{P,k} \omega_k}{b_{P,k}^2} \left(1 - \frac{\Delta \theta_{P,k}^2}{2b_{P,k}^2}\right) \exp\left(\frac{-\Delta \theta_{P,k}^2}{2b_{P,k}^2}\right) \\
 D_k(3, 16) &= -\delta \frac{\alpha_{P,k} \Delta \theta_{P,k}}{b_{P,k}^2} \exp\left(\frac{-\Delta \theta_{P,k}^2}{2b_{P,k}^2}\right) \\
 D_k(5, 2 : 4) &= -\delta \frac{\omega_k \Delta \theta_{ik}}{b_{ik}^2} \exp\left(\frac{-\Delta \theta_{ik}^2}{2b_{ik}^2}\right), \quad i \in \{Q, R, S\} \\
 D_k(5, 7 : 9) &= 2\delta \frac{\alpha_{ik} \omega_k \Delta \theta_{ik}}{b_{ik}^3} \left(1 - \frac{\Delta \theta_{ik}^2}{2b_{ik}^2}\right) \exp\left(\frac{-\Delta \theta_{ik}^2}{2b_{ik}^2}\right), \quad i \in \{Q, R, S\} \\
 D_k(5, 12 : 14) &= \delta \frac{\alpha_{ik} \omega_k}{b_{ik}^2} \left(1 - \frac{\Delta \theta_{ik}^2}{2b_{ik}^2}\right) \exp\left(\frac{-\Delta \theta_{ik}^2}{2b_{ik}^2}\right), \quad i \in \{Q, R, S\} \\
 D_k(5, 16) &= -\sum_{i \in \{Q, R, S\}} \delta \frac{\alpha_{ik} \Delta \theta_{ik}}{b_{ik}^2} \exp\left(\frac{-\Delta \theta_{ik}^2}{2b_{ik}^2}\right) \\
 D_k(7, 5) &= -\delta \frac{\omega_k \Delta \theta_{T,k}}{b_{T,k}^2} \exp\left(\frac{-\Delta \theta_{T,k}^2}{2b_{T,k}^2}\right) \\
 D_k(7, 10) &= 2\delta \frac{\alpha_{T,k} \omega_k \Delta \theta_{T,k}}{b_{T,k}^3} \left(1 - \frac{\Delta \theta_{T,k}^2}{2b_{T,k}^2}\right) \exp\left(\frac{-\Delta \theta_{T,k}^2}{2b_{T,k}^2}\right) \\
 D_k(7, 15) &= \delta \frac{\alpha_{T,k} \omega_k}{b_{T,k}^2} \left(1 - \frac{\Delta \theta_{T,k}^2}{2b_{T,k}^2}\right) \exp\left(\frac{-\Delta \theta_{T,k}^2}{2b_{T,k}^2}\right) \\
 D_k(7, 16) &= -\delta \frac{\alpha_{T,k} \Delta \theta_{T,k}}{b_{T,k}^2} \exp\left(\frac{-\Delta \theta_{T,k}^2}{2b_{T,k}^2}\right)
 \end{aligned} \tag{A.2}$$

Appendix B. Functions of switching Kalman filter

1. $[\underline{x}_k^{ij}, P_k^{ij}, L_k^{ij}] = filter(\underline{x}_{k-1}^i, P_{k-1}^i, A_k, D_k, Q_k, H_k^{(j)}, R_k^{(j)})$
 In this function at each time k , first a *a priori* estimate and its covariance matrix (\underline{x}_k^{ij} and P_k^{ij}) are estimated from the previous time $k - 1$. Then, by using the estimate \underline{x}_k^{ij} and observation y_k , the estimate is updated and the posterior estimate and its covariance (\underline{x}_k^{ij} and P_k^{ij}) are computed. In this function, e_k is the innovation at time k . The likelihood L_k^{ij} is the probability of the observation y_k and can be calculated as a by-product of Kalman filter. Finally, b_k is the Kalman gain matrix.

$$\begin{cases}
 \underline{x}_k^{ij} = A_k \underline{x}_{k-1}^i \\
 P_k^{ij} = A_k P_{k-1}^i A_k^T + D_k Q_k D_k^T \\
 e_k = y_k - H_k^{(j)} \underline{x}_k^{ij} \\
 L_k^{ij} = \mathcal{N}(e_k; 0, H_k^{(j)} P_k^{ij} H_k^{(j)T} + R_k^{(j)}) \\
 b_k = P_k^{ij} H_k^{(j)T} [H_k^{(j)} P_k^{ij} H_k^{(j)T} + R_k^{(j)}]^{-1} \\
 P_k^{ij} = [I - b_k H_k^{(j)}] P_k^{ij} \\
 \underline{x}_k^{ij} = \underline{x}_k^{ij} + b_k [y_k - H_k^{(j)} \underline{x}_k^{ij}]
 \end{cases} \tag{B.1}$$

2. $[K_k^{ij}, K_k^j, g_k^{ij}] = StatesProbability(L_k^{ij}, z_{ij}, K_{k-1}^i)$

This function calculates the parameter K_k^j for each mode j at time k .

$$\begin{cases}
 i, j = 1, 2, \dots, 7 \\
 K_k^{ij} = \frac{L_k^{ij} z_{ij} K_{k-1}^i}{\sum_i \sum_j L_k^{ij} z_{ij} K_{k-1}^i} \\
 K_k^j = \sum_i K_k^{ij} \\
 g_k^{ij} = \frac{K_k^{ij}}{K_k^j}
 \end{cases} \tag{B.2}$$

3. $[\underline{x}_k^j, P_k^j] = Collapse(\underline{x}_k^{ij}, P_k^{ij}, K_k^j, g_k^{ij})$

This function approximates mixture of Gaussians as one Gaussian by moment matching.

$$\begin{cases}
 \underline{x}_k^j = \sum_i \underline{x}_k^{ij} g_k^{ij} \\
 P_k^j = g_k^{ij} [P_k^i + (\underline{x}_k^{ij} - \underline{x}_k^j)(\underline{x}_k^{ij} - \underline{x}_k^j)^T]
 \end{cases} \tag{B.3}$$

References

- [1] B. Kohler, C. Hennig, R. Orglmeister, The principles of software QRS detection: Reviewing and comparing algorithms for detecting this important ECG waveform, *IEEE Eng. Med. Biol.* 2 (2002) 42–57.
- [2] B.C. Yu, S. Liu, M. Lee, C.Y. Chen, B.N. Chiang, A nonlinear digital filter for cardiac QRS complex detection, *J. Clin. Eng.* 10 (1985) 193–201.
- [3] E. Soria, M. Sober, J. Calpe, J. Francisco, J. Chorro, J. Lopez, Application of adaptive signal processing for determining the limits of P and T waves in an ECG, *IEEE Trans. Biomed. Eng.* 45 (8) (1998) 1077–1080.
- [4] Y.H. Hu, W.J. Tompkins, J.L. Urrusti, V.X. Afonso, Applications of artificial neural networks for ECG signal detection and classification, *J. Electrocardiol.* 26 (1993) 66–73.
- [5] S.S. Mehta, N.S. Lingayat, Combined entropy based method for detection of QRS complexes in 12-lead electrocardiogram using SVM, *Comput. Biol. Med.* 38 (2008) 138–145.
- [6] S.S. Mehta, C.R. Trivedi, N.S. Lingayat, Identification and delineation of QRS complexes in electrocardiogram using fuzzy C-means algorithm, *J. Theor. Appl. Inf. Technol.* 5 (5) (2009) 609–617.
- [7] M. Merah, T.A. Abdelmalik, B.H. Larbi, R-peaks detection based on stationary wavelet transform, *Comput. Methods Programs Biomed.* 121 (2015) 149–160.
- [8] S. Pal, M. Mitra, Empirical mode decomposition based ECG enhancement and QRS detection, *Comput. Biol. Med.* 42 (2012) 83–92.
- [9] P. Laguna, R. Jane, R. Caminal, Automatic detection of wave boundaries in multi-lead ECG signals: validation with the CSE data-base, *Comput. Biomed. Res.* 27 (1994) 45–60.
- [10] D.A. Coast, R.M. Stern, G.G. Cano, S.A. Briller, An approach to cardiac arrhythmia analysis using hidden Markov models, *IEEE Trans. Biomed. Eng.* 37 (9) (1990) 826–836.
- [11] N.P. Hughes, Probabilistic Models for Automated ECG Interval Analysis, Ph.D. thesis, Department of Engineering Science, University of Oxford, 2006.
- [12] R. Andreato, B. Dorizzi, J. Boudy, ECG Signal analysis through hidden Markov models, *IEEE Trans. Biomed. Eng.* 53 (8) (2006) 1541–1549.
- [13] R. Andreato, J. Boudy, Combining wavelet transform and hidden Markov models for ECG segmentation, *EURASIP J. Adv. Signal Process.* 2007 (2006) 1–6.
- [14] M. Akhbari, M.B. Shamsollahi, O. Sayadi, A.A. Armoundas, C. Jutten, ECG Segmentation and fiducial point extraction using multi hidden Markov model, *Comput. Biol. Med.* 79 (2016) 21–29.
- [15] C. Lin, C. Mailhes, J.Y. Tournier, P- and T-wave delineation in ECG signals using a Bayesian approach and a partially collapsed Gibbs sampler, *IEEE Trans. Biomed. Eng.* 57 (12) (2010) 2840–2849.
- [16] C. Li, C. Zheng, C. Tai, Detection of ECG characteristic points using wavelet transforms, *IEEE Trans. Biomed. Eng.* 42 (1) (1995) 21–28.
- [17] J.P. Martinez, R. Almeida, S. Olmos, A.P. Rocha, P. Laguna, A wavelet-based ECG delineator: evaluation on standard databases, *IEEE Trans. Biomed. Eng.* 51 (4) (2004) 570–581.
- [18] J. Dumont, A.I. Hernandez, G. Carraut, Improving ECG beats delineation with an evolutionary optimization process, *IEEE Trans. Biomed. Eng.* 57 (2010) 607–615.
- [19] M.R. Homaeinezhad, M.E. Moshiri-Nejad, H. Naseri, A correlation analysis-based detection and delineation of ECG characteristic events using template waveforms extracted by ensemble averaging of clustered heart cycles, *Comput. Biol. Med.* 44 (2014) 66–75.
- [20] A. Karimipour, M.R. Homaeinezhad, Real-time electrocardiogram P-QRS-T detection-delineation algorithm based on quality-supported analysis of characteristic templates, *Comput. Biol. Med.* 52 (2014) 153–165.
- [21] M. Akhbari, M.B. Shamsollahi, C. Jutten, Fiducial points extraction and characteristic waves detection in ECG signal using a model-based Bayesian framework, in: *Proceedings of the 2013 International Conference on Acoustics, Speech, and Signal Processing*, 2013, pp. 1257–1261.

- [22] O. Sayadi, M.B. Shamsollahi, A model-based Bayesian framework for ECG beat segmentation, *Physiol. Meas.* 30 (2009) 335–352.
- [23] M. Akhbari, M.B. Shamsollahi, C. Jutten, ECG fiducial points extraction by extended Kalman filtering, in: *Proceedings of the 2013 International Conference on Telecommunications and Signal Processing*, 2013, pp. 628–632.
- [24] M. Akhbari, M.B. Shamsollahi, C. Jutten, A.A. Armoundas, O. Sayadi, ECG denoising and fiducial point extraction using extended Kalman filtering framework with linear and nonlinear phase observation, *Physiol. Meas. J.* 37 (2016) 203–226.
- [25] S. Maheshwari, A. Acharyya, P.E. Puddu, E.B. Mazomenos, G. Leekha, K. Maharatna, M. Schiariti, An automated algorithm for online detection of fragmented QRS and identification of its various morphologies, *J. R. Soc.* 10 (2013) 1–18.
- [26] E.B. Mazomenos, D. Biswas, A. Acharyya, T. Chen, K. Maharatna, J. Rosengarten, J. Morgan, N. Curzen, A low-complexity ECG feature extraction algorithm for mobile healthcare applications, *IEEE J. Biomed. Health Inform.* 17 (2013) 459–469.
- [27] V. Bono, E.B. Mazomenos, T. Chen, J.A. Rosengarten, A. Acharyya, K. Maharatna, J.M. Morgan, N. Curzen, Development of an automated updated selvester QRS scoring system using SWT-based QRS fractionation detection and classification, *IEEE J. Biomed. Health Inform.* 18 (2014) 193–204.
- [28] A. Kumar, M. Singh, Ischemia detection using isoelectric energy function, *Comput. Biol. Med.* 68 (2016) 76–83.
- [29] F. Gargiulo, A. Fratini, M. Sansone, C. Sansone, Subject identification via ECG fiducial-based systems: influence of the type of QT interval correction, *Comput. Methods Programs Biomed.* 121 (2015) 127–136.
- [30] S. Barra, A. Casanova, M. Fraschini, M. Nappi, EEG/ECG signal fusion aimed at biometric recognition, in: *Proceedings of the 2015 ICIAP International Workshops, BioFor, CTMR, RHEUMA, ISCA, MADiMa, SBMI, and QoEM*, 2015, pp. 35–42.
- [31] S. Barra, A. Casanova, M. Fraschini, M. Nappi, Fusion of physiological measures for multimodal biometric, *Multimed. Tools Appl.* 76 (2016) 1–13.
- [32] Z. Ghahramani, G.E. Hinton, Variational learning for switching state-space models, *Tech. rep.*, Neural Computation, 1998.
- [33] K.P. Murphy, Switching Kalman Filters, *Technical report*, Citeseer, 1998.
- [34] Z. Ghahramani, G.E. Hinton, Switching state space models, *Tech. rep.*, Neural Computation, 1998.
- [35] V. Pavlovic, J.M. Rehg, T. Cham, K.P. Murphy, A dynamic Bayesian network approach to figure tracking using learned dynamic models, in: *Proceedings of the 1999 IEEE International Conference on Computer Vision*, 1999, pp. 94–101.
- [36] Y. Zheng, M. Hasegawa-Johnson, Acoustic segmentation using switching state Kalman filter, in: *Proceedings of the 2003 IEEE International Conference on Acoustics, Speech, and Signal Processing*, 2003, pp. 752–755.
- [37] Y. Wu, G. Hua, T. Yu, Switching observation models for contour tracking in clutter, in: *Proceedings of the 2003 IEEE Conference on Computer Vision and Pattern Recognition*, 2003.
- [38] W. Wu, M.J. Black, D. Mumford, Y. Gao, E. Bienenstock, J.P. Donoghue, Modeling and decoding motor cortical activity using a switching Kalman filter, *IEEE Trans. Biomed. Eng.* 51 (6) (2004) 933–942.
- [39] V. Manfredi, S. Mahadevan, J.F. Kurose, Switching Kalman filters for prediction and tracking in an adaptive meteorological sensing network, in: *Proceedings of the 2005 IEEE Conference on Sensor and Ad Hoc Communications and Networks*, 2005, pp. 197–206.
- [40] H. Veeraraghavan, P. Schrater, N. Papanikolopoulos, Switching Kalman filter-based approach for tracking and event detection at traffic intersections, in: *Proceedings of the 2005 Mediterranean Conference on Control and Automation*, 2005, pp. 1167–1172.
- [41] J. Oster, J. Behar, O. Sayadi, S. Nemati, A.E.W. Johnson, G.D. Clifford, Semi-supervised ECG ventricular beat classification with novelty detection based on switching Kalman filters, *IEEE Trans. Biomed. Eng.* 62 (9) (2015) 2125–2134.
- [42] N. Montazeri, M.B. Shamsollahi, D. Ge, A.I. Hernandez, Switching Kalman filter based methods for apnea bradycardia detection from ECG signals, *Physiol. Meas.* 36 (9) (2015) 1763–1783.
- [43] P.E. McSharry, G.D. Clifford, L. Tarassenko, L.A. Smith, A dynamic model for generating synthetic electrocardiogram signals, *IEEE Trans. Biomed. Eng.* 50 (3) (2003) 289–294.
- [44] <http://www.physionet.org/physiobank/database/qtddb>.
- [45] P. Laguna, R.G. Mark, A. Goldberg, G.B. Moody, A database for evaluation of algorithms for measurement of QT and other waveform intervals in the ECG, *IEEE Comput. Cardiol.* 24 (1997) 673–676.
- [46] R. Sameni, M.B. Shamsollahi, C. Jutten, G.D. Clifford, Nonlinear Bayesian filtering framework for ECG denoising, *IEEE Trans. Biomed. Eng.* 54 (12) (2007) 2172–2185.
- [47] R. Kohavi, A study of cross validation and bootstrap for accuracy estimation and model selection, in: *Proceedings of the 1995 International Joint Conference on Artificial Intelligence*, 1995.
- [48] J. Behar, J. Oster, G.D. Clifford, Combining and benchmarking methods of foetal ECG extraction without maternal or scalp electrode data, *Physiol. Meas.* 35 (2014) 1569–1589.